NON-PREMIXED COUNTERFLOW FLAMES INSIDE A FLAT PLATE CHANNEL WITH RECTANGULAR OBSTRUCTIONS

Antonio Pereira Roseira Junior, aroseira@ctex.eb.br
Centro Tecnológico do Exército - Seção de Mísseis e Foguetes/ Divisão Bélica - 23020-470 - Rio de Janeiro - RJ - Brazil

Aldélio Bueno Caldeira, aldelio@ime.eb.br
Instituto Militar de Engenharia - Seção de Engenharia Mecânica e de Materiais - SE/4 - 22290-270 - Rio de Janeiro - RJ - Brazil

Abstract. *Non-premixed counterflow flames inside a parallel flat plate channel with rectangular obstructions are studied by a numerical approach. The oxidant and the fuel enter in the channel through different slots positioned on each channel wall. In the entrance region of the channel, a counterflow is formed. Downstream, rectangular symmetric obstructions are positioned on the channel walls. The obstructions and the walls are adiabatic. The model is based on mass, momentum and mixture fraction conservation equations, considering the Simple Chemical Reaction mechanism. The incompressible laminar flow governing equations, written in vorticity-stream function formulation, and the mixture fraction conservation equation are discretized with a BTCS finite difference scheme. A parametric study is conducted for Reynolds number and obstruction dimensions. The influences of the dimensions and the position of the obstructions on the flame behavior and the vortex/flame interaction are analyzed. The results show the flame shape, temperature fields and stream function fields.*

Keywords*: non-premixed counterflow flame, obstruction, mixture fraction*

1. INTRODUCTION

"Opposing jet impacting head-on provide a simple in-line mixer configuration with potential industrial applications for rapid mixing of viscous fluids" (Wang *et al*., 2005). "Compared with mechanically agitated mixers, mixers which use the opposing jet technique to create high turbulence, high shear rates and vortex motion caused by collision of the opposing jets offer several advantages in achieving rapid mixing over a short distance in the mixing chamber without use of moving parts of internal baffles" (Wang and Mujumdar, 2006).

The vortex/flame interaction is an important phenomenon in reacting flows. The vortexes zones improve the mixing and the residence time. Furthermore, a simple way of generating vortex zones (or recirculation zones) is based on the introduction of obstructions in the flow. The geometry and thermo-physical properties of these obstructions are relevant parameters on momentum, heat and mass transfer process, modifying the dimensions and the positions of the hot and cold zones of the flow (Caldeira, *et al.*, 2001, 2002, 2005, Esquiva-Dano *et al*., 2001, 2005).

The counterflow configuration is a commonly used geometry for experimental combustion and chemical kinetic modeling studies of non-premixed combustion. Works on interaction of laminar vortexes generated from either the fuel side or the oxidizer side (Santoro *et al*, 1999), flame-extinction phenomena (Pellet *et al*, 1998, Daou and Liñán, 1999), and on the modeling of vortex-flame interactions (Amantini *et al*, 2006) are such examples of this usage. However, the counterflow can also be found in non-combustion problems. Hosseinalipour and Mujumdar (1997) developed the first numerical model for two-dimensional confined opposing jets with either isothermal or adiabatic walls in steady laminar flow. The concept involved dividing one of the fluid streams into a multiplicity of streams, which were injected into the main flow channel as two-dimensional slot jets, which were directed in opposite directions. Also, Wang *et al* (2005) reported numerical studies with new design approaches to improve mixing effectiveness under laminar conditions in two-dimensional laminar confined opposing streams. Since the improvement of mixing effectiveness was found to depend strongly on the operating conditions and geometric configurations, they were motivated to investigate the addition of baffles along the channel, which is beneficial to enhance mixing effectiveness.

The counterflow flame is also found in studies on the overall reaction rates for fuel-oxidant combinations, the effectiveness of inhibitors (Tsuji, 1982), the transient phenomena during diffusion/edge flame transition (Frouzakis *et al*, 2002) and the burning of multicomponent fuels in a diffusion flame (Fachini, 2001, 2004). Furthermore, in confined reacting counterflow, the vortex/flame interaction is also important. Due to the presence of the solid channel or duct walls, a significant recirculation zone is produced (Roseira Jr and Leiroz, 2005).

In present work, the combustion problem involving a non-premixed flame in modified two-dimensional counterflow geometry of slot burners is studied by a numerical approach. Adiabatic solid walls are placed beside the counterflow, creating a parallel flat plate channel. Symmetric rectangular obstructions are positioned on the solid walls. The influences of the dimensions and the position of the obstructions on the flame behavior and the vortex/ flame interaction are analyzed. The results show the flame shape, temperature fields and stream function fields.

2. PHYSICAL AND MATHEMATICAL MODEL

The physical model involves the combustion of two initially separate streams of fuel and oxidizer in gas-phase in a steady two-dimensional confined laminar opposing jets. The oxidant and the fuel enter in the channel through different slots positioned on each channel wall. In the entrance region of the channel, a counterflow is formed. The configuration is commonly used in numerical and analytical studies since results are easily verified experimentally due to the easy access in the flame region (Fachini, 2001). The thermo-physical properties are assumed constant. In order to solve the Navier-Stokes equations, the Vorticity-Stream function formulation is employed, eliminating the pressure as a dependent variable from the momentum conservation equations and reducing the number of equations to be solved simultaneously. The continuity equation is identically satisfied by the stream function definition. The Vorticity-Stream function formulation presents a difficulty in the specification of vorticity boundary conditions. It is necessary to specify vorticity values along the solid boundaries in terms of the stream function, which requires the discretization using second order derivatives. Along the symmetry plane, zero-vorticity boundary condition is applied.

The Simple Chemical Reaction System hypothesis is employed and the values of diffusivities of mass and energy are considered equal for each species. The mathematical model is based on the mass, momentum and mixture fraction conservation equations. The manipulation procedures done in the fluid dynamic and thermo-chemistry systems can be found in Anderson *et al* (1984) and Kuo (1986).

The geometry adopted to represent the physical half-domain is described in a Cartesian system of coordinates by four boundaries (Fig.1). The left boundary represents the flow field symmetry plane and the nozzle separation width (L^*), the right boundary is the outflow region, as well as the truncation position in the horizontal direction. The top and bottom boundaries (P^*) include the fuel and oxidizer nozzles widths, respectively, D_F^* and D_O^*, and the solid walls (with the solid obstructions), which are adiabatic and nonreactive. The symmetric rectangular solid obstructions are positioned at a distance P^*_{obs} from the left boundary. The obstructions thickness and height are respectively L^*_{obs} and H^*_{obs}.

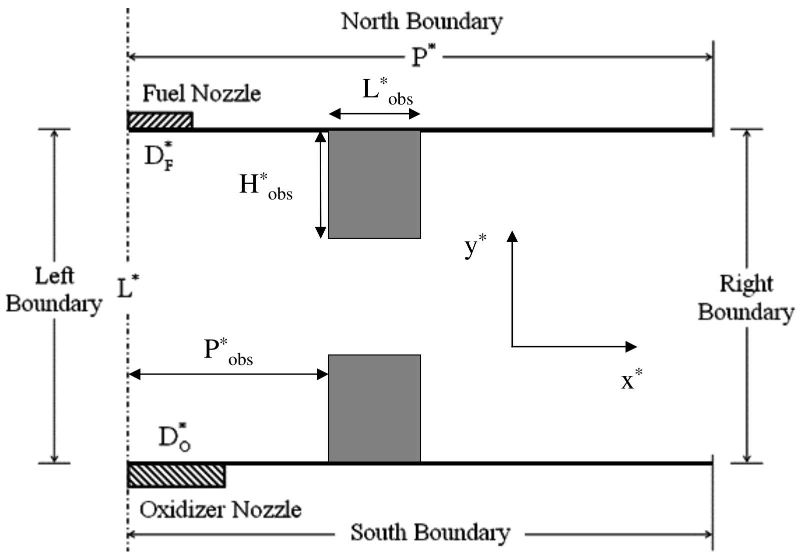

Figure 1. Geometry adopted representing a half-domain.

The definitions of the dimensionless groups employed in the following equations are given by Eqs. 1.a-j.

$$x = \frac{x^*}{D_F^*} \; ; \; y = \frac{y^*}{D_F^*} \; ; \; L = \frac{L^*}{D_F^*} \; ; \; P = \frac{P^*}{D_F^*} \; ; \; u = \frac{u^*}{|U_F^*|} \; ; \; v = \frac{v^*}{|U_F^*|}$$
$$\omega = \frac{\omega^* D_F^*}{|U_F^*|} \; ; \; \psi = \frac{\psi^*}{|U_F^*|.D_F^*} \; ; \; t = \frac{t^* |U_F^*|}{D_F^*} \; ; \; \theta = \frac{T^* - T_F}{T_O - T_F} \qquad (1.a\text{-}j)$$

where U_F^* is the fuel peak velocity (at the top nozzle) and, T_F, T_O the respective fuel and oxidizer inflow temperatures.

The fluid dynamic system is described by the Navies-Stokes equations: mass and momentum conservation equations. However, by introducing the Vorticity-Stream function formulation, we can manipulate the momentum equations and use the definition of vorticity as

$$\omega = \frac{\partial v}{\partial x} - \frac{\partial u}{\partial y}, \tag{2}$$

which results in a Vorticity Transport equation

$$\frac{\partial \omega}{\partial t} + u\frac{\partial \omega}{\partial x} + v\frac{\partial \omega}{\partial y} = \frac{1}{Re}\left(\frac{\partial^2 \omega}{\partial x^2} + \frac{\partial^2 \omega}{\partial y^2}\right) \tag{3}$$

The Reynolds number is defined based on the fuel nozzle

$$Re = \frac{\left|U_F^*\right|.D_F^*}{\upsilon} \quad ; \quad \upsilon \text{ is the fuel kinematic viscosity.} \tag{4}$$

Stream function $\psi(x,y)$ is defined, using the velocity components in order to satisfy the continuity equation, as

$$u = \frac{\partial \psi}{\partial y} \quad ; \quad v = -\frac{\partial \psi}{\partial x} \tag{5.a-b}$$

Replacing the velocity components Eqs.(5.a-b) in Eq.(2), we obtain the Poisson's equation for the stream function.

$$-\omega = \frac{\partial^2 \psi}{\partial x^2} + \frac{\partial^2 \psi}{\partial y^2} \tag{6}$$

The parabolic velocity profile was used to represent the inflow velocity conditions at the nozzles and at the outflow boundaries. Therefore, the velocities boundary conditions must be expressed in terms of stream function, as:

$$\begin{aligned}
&\psi = 0 \quad ; \quad x = 0\ ,\ 0 < y < \frac{1}{R_{DL}} \\
&\psi(x) = \frac{3x}{2}\left(1 - \frac{x^2}{3}\right) \quad ; \quad 0 \le x \le 1\ ,\ y = \frac{1}{R_{DL}} \\
&\psi = 1 \quad ; \quad 1 < x \le R_H\ ,\ y = \frac{1}{R_{DL}} \\
&\psi(y) = y^2 R_{DL}{}^2 (1 + R_V.R_B)(3 - 2yR_{DL}) - R_V.R_B \quad ; \quad x = R_H\ ,\ 0 < y < \frac{1}{R_{DL}} \\
&\psi(x) = -\frac{3xR_V}{2}\left[1 - \frac{1}{3}\left(\frac{x}{R_B}\right)^2\right] \quad ; \quad 0 \le x \le R_B\ ,\ y = 0 \\
&\psi = -R_V.R_B \quad ; \quad R_B < x \le R_H\ ,\ y = 0
\end{aligned} \tag{7.a-f}$$

The following dimensionless ratios represent, respectively, the fuel nozzle width-separation distance, the horizontal aspect, inflow peak velocities, and nozzle width ratios.

$$R_{DL} = \frac{D_F^*}{L^*},\quad R_H = \frac{P^*}{D_F^*},\quad R_V = \frac{U_O^*}{\left|U_F^*\right|},\quad R_B = \frac{D_O^*}{D_F^*} \tag{8}$$

The thermo-chemistry system is described by the energy and chemical species equations:

$$\frac{\partial \theta}{\partial t} + u\frac{\partial \theta}{\partial x} + v\frac{\partial \theta}{\partial y} = \frac{1}{Pe}\left(\frac{\partial^2 \theta}{\partial x^2} + \frac{\partial^2 \theta}{\partial y^2}\right) + \frac{\dot{\omega}_F^*\,\Delta H_C}{\rho c_p (T_O - T_F)}.\frac{D_F^*}{\left|U_F^*\right|} \tag{9}$$

$$\frac{\partial Y_i}{\partial t}+u\frac{\partial Y_i}{\partial x}+v\frac{\partial Y_i}{\partial y}=\frac{1}{Pe\,Le_i}\left(\frac{\partial^2 Y_i}{\partial x^2}+\frac{\partial^2 Y_i}{\partial y^2}\right)-\frac{D_F^*}{\left|U_F^*\right|}\frac{\dot{\omega}_i^*}{\rho} \tag{10.a-b}$$

where α is the thermal diffusivity, ΔH_C is the heat release rate and $Y_i^*, \dot{\omega}_i^*$ are, respectively, the mass fraction in the mixture and consumption rate of the "i" specie. The mass diffusivity coefficients are considered equal for each species ($D_{ij}=D_{ji}=D$). The Simple Chemical Reaction System (SRCS) hypothesis is employed and the mixture fraction conservation equation can be obtained by following the assumption:

$$1 \text{ kg of Fuel} + s \text{ kg of Oxidizer} \longrightarrow (1+s) \text{ kg of Products} \tag{11}$$

For stoichiometric coefficients, n_F, n_o, and molecular weights of fuel and oxidizer, W_F, W_o, the mass-weighted stoichiometric coefficient ratio (s) can be written as:

$$s=\frac{n_O.W_O}{n_F.W_F} \tag{12}$$

As consequence, the species consumption rates can be written as:

$$\dot{\omega}_F^*=\frac{\dot{\omega}_O^*}{s} \tag{13}$$

Assuming $Le_1 = Le_2 = 1$ and manipulating the species equations (Eqs. 10.a-b), the first coupling variable and the correspondent conservation equation can be established as follows by:

$$\phi_{FO}=Y_F-\frac{Y_O}{s} \tag{14}$$

$$\frac{\partial \phi_{FO}}{\partial t}+u\frac{\partial \phi_{FO}}{\partial x}+v\frac{\partial \phi_{FO}}{\partial y}=\frac{1}{Pe}\left(\frac{\partial^2 \phi_{FO}}{\partial x^2}+\frac{\partial^2 \phi_{FO}}{\partial y^2}\right) \tag{15}$$

In a similar way, the other two coupling variables and the dimensionless heat release rate (Q) can be expressed as:

$$\phi_{TF}=Q.Y_F+\theta \quad ; \quad \phi_{TO}=\frac{Q.Y_O}{s}+\theta \quad \text{and} \quad Q=\frac{\Delta H_C}{c_p(T_O-T_F)} \;, \tag{16.a-c}$$

resulting in a linear relation among the coupling variables:

$$\phi_{TO}=\phi_{TF}-Q.\phi_{FO} \tag{17}$$

Summarizing, the boundary condition for the fluid dynamics problem is the null velocity at solid boundaries, null tension at the left and right boundaries and prescribed inlet velocities *v* at nozzles with *u* equal to zero. For the heat and mass transfer problem, the boundary condition is the null diffusion flux along the solid walls and along the left and right boundaries. But at the fluid inlet, the mass fraction of the fuel is equal to one and the dimensionless temperature is zero at fuel nozzle, while at oxidant nozzle the mass fraction of the oxidant is equal to one and the dimensionless temperature is equal to one. The initial condition is the stagnant, isothermal and inert medium.

3. NUMERICAL PROCEDURE

The Finite-Difference Method is employed on the resulting conservation equations, which are discretized using the BTCS (Backward in Time Centered in Space) scheme (Anderson *et al*, 1984). An iterative numerical technique, based on the algorithm of the Gauss-Seidel with successive under-relaxation and local error control is applied to solve the resulting algebraic linear systems. A non-uniform structured mesh is employed with 161 x 41 points.

4. RESULTS

The proposed configuration of the confined counterflow with obstructions joins two important mechanisms. The first mechanism is the vortexes zones created after the obstructions and the second mechanism is the adiabatic blockage introduced by the presence of the obstructions. Furthermore, for small Reynolds number and for obstructions with high values of height the flame is confined before the obstruction.

The results section is divided in three subsections, the first one is devoted to the analysis of vortex zones, the second one is dedicated to the analysis of the Reynolds number on flame behavior, and the third one reports the analysis of the obstruction geometry, considering small Reynolds number, on the flame and temperature fields.

4.1. Vortex zones analysis

The geometry of the obstruction analyzed is this subsection is defined by $P^*_{obs} = 2$, $H^*_{obs} = 0.5$ and $L^*_{obs} = 0.5$. The inlet flow and physical parameters are Prandtl number, Pr = 0.7, inlet velocity ratio, $R_V = 1$ and $R_B = 1$, fuel nozzle length, $D^*_F = 1$, and distance between the nozzles, $L^* = 2$. The thermo-physical properties are chosen as $\Delta H_C = 802$ kJ/mol (Kuo, 1986); $c_p = 30$ J/mol.K; $T_O = 400$ K; $T_F = 300$ K; $Y_{O,in} = 0.233$; $Y_{F,in} = 1$ and $\phi^*_{FO,St} = 0.05518$. The specific heat at constant pressure was considered constant at the average value between the air and the fuel at the nozzles temperatures (Fachini, 2004).

The Figs (2) and (3) show the stream function fields for Re = 10 and for Re = 80. Comparing these figures is possible to note the presence of the vortexes zones for Re = 80 (dash dotted lines), but for Re = 10 those zones are not present. So, for small Reynolds number there are not the eddy zones after the obstructions. Otherwise, for high values of Reynolds the intense vortex regions are created.

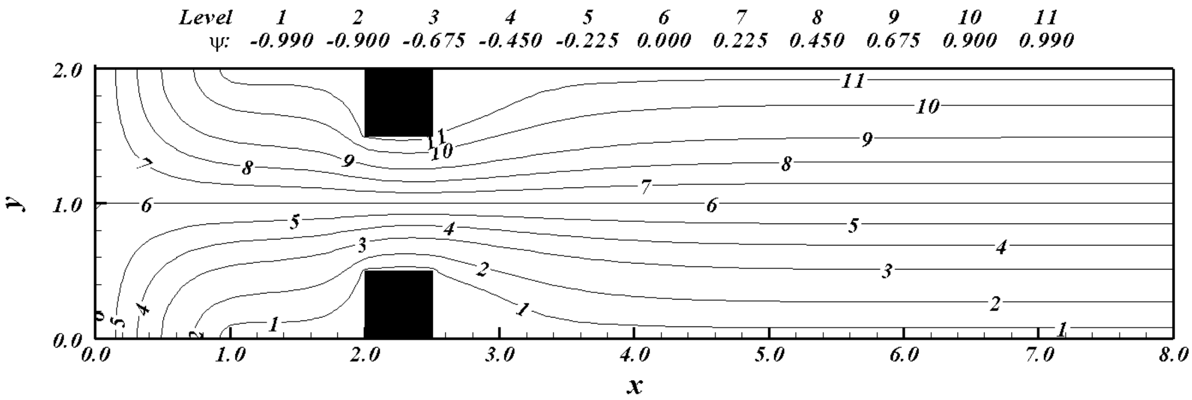

Figure 2. Stream function field (Re = 10).

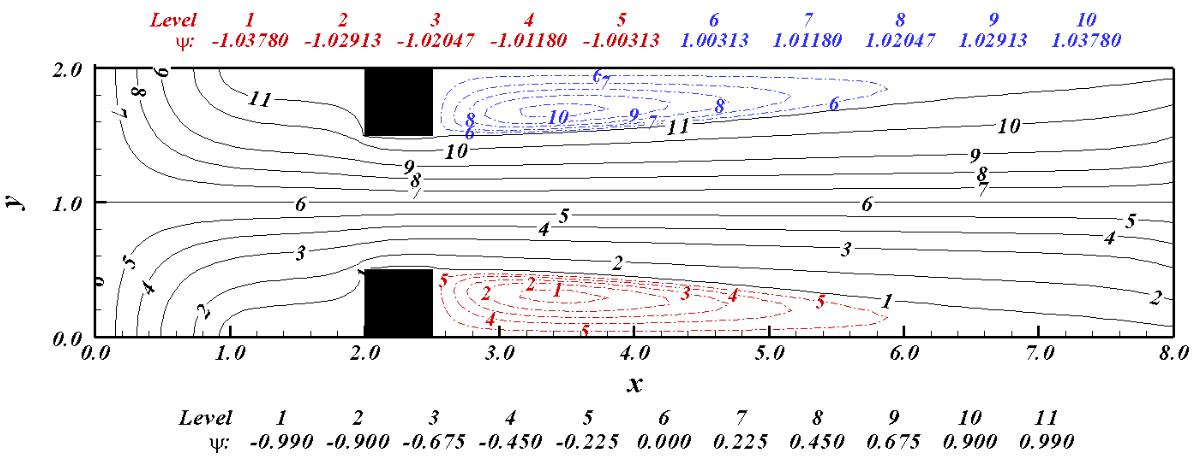

Figure 3. Stream function field (Re = 80).

The temperature fields in the proposed problem indicate the flame behavior and furnish information about the hottest and coldest regions inside the channel. In Figs. (4) and (5) the temperature fields for the cases with Re = 10 and Re = 80 are shown.

The black solid line represents the stoichiometric relation for the first conserved scalar, Eq.(14), where the combustion reaction takes place, indicating the flame position. Therefore, an underventilated flame can be observed, touching the bottom wall before the obstruction, at the x = 1.2 coordinate. The flame is located next to the oxidizer nozzle (bottom) and also below the stagnation plane of the flow field (y = 1.0). The hottest zone is linked with the flame position and the coldest one can be observed faraway from the flame. Therefore, increasing the Reynolds number the flame reaches greater channel lengths.

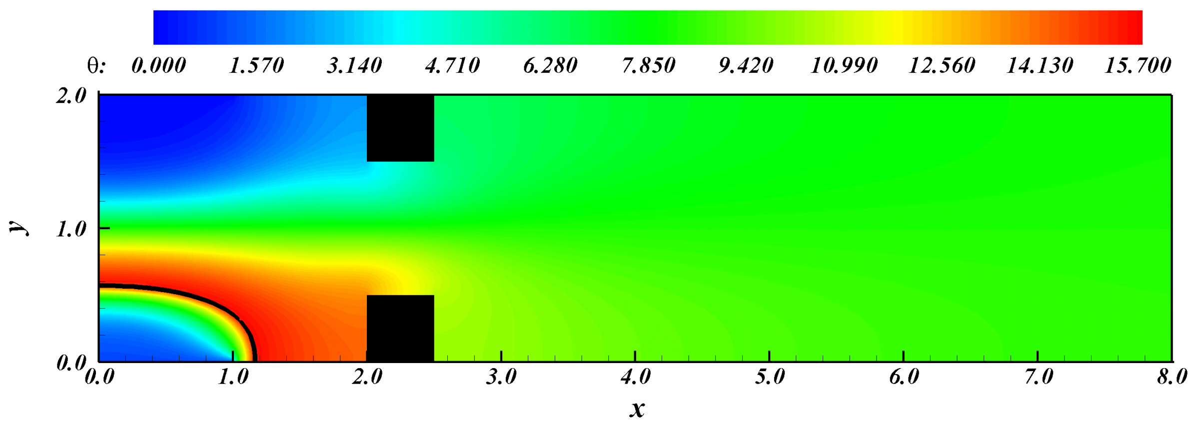

Figure 4. Temperature field (Re = 10).

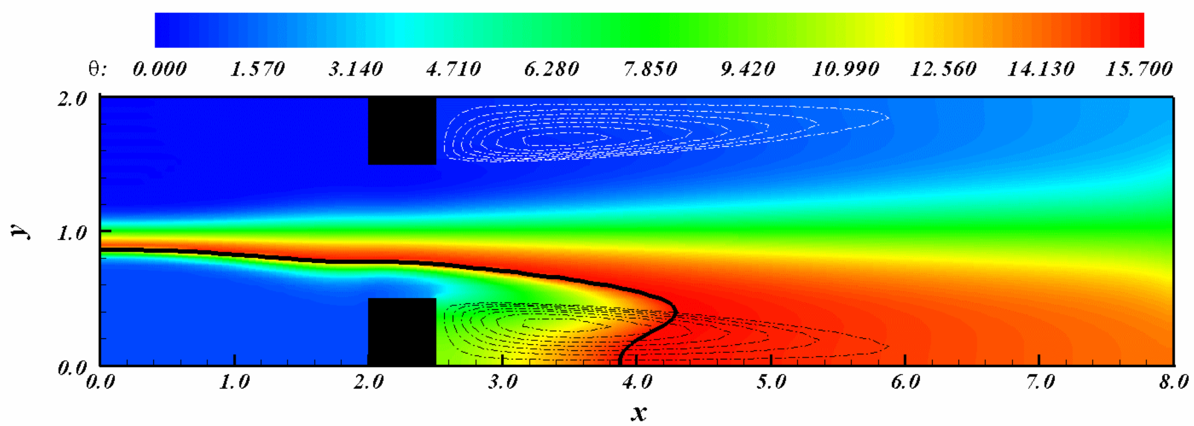

Figure 5. Temperature field (Re = 80).

4.2. Reynolds number analysis

In this subsection, the cases analyzed takes account the same values of the parameters employed in the subsection 4.1. However, the focus of the present investigation is the Reynolds number and the obstructions effects on flame behavior.

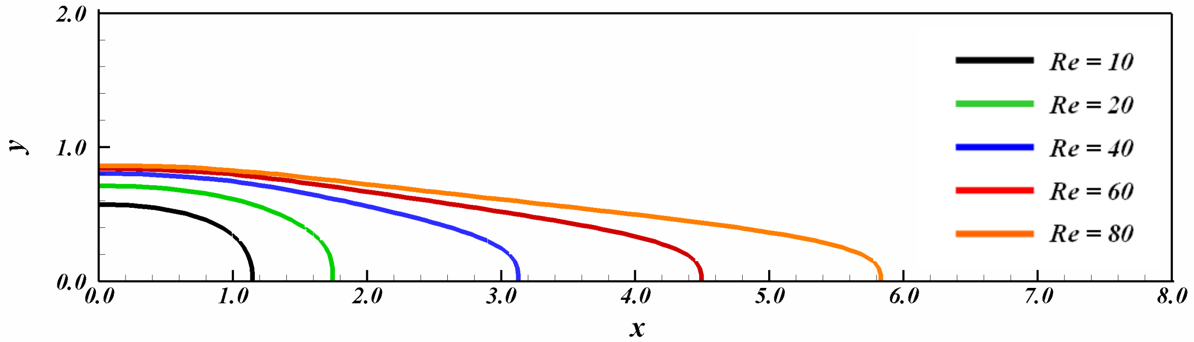

Figure 6. Flame Behavior without obstructions.

Comparing the Figs (6) and (7) the relevance of the obstructions in reducing the flame length is shown for Reynolds number greater than 20. For these cases, the eddy zones and the physical geometry of the obstruction keep the flame in short channel lengths. The vortexes zones deform the flame, as can be seen in Fig. (7) for Re = 60 and Re = 80. Outside the vortexes zones the flame reaches greater distances along the channel.
This phenomenon shows the relation between the eddy zone and the obstructions. However, for low Reynolds number ($Re \leq 20$) the obstructions confined the flame before the obstructions.

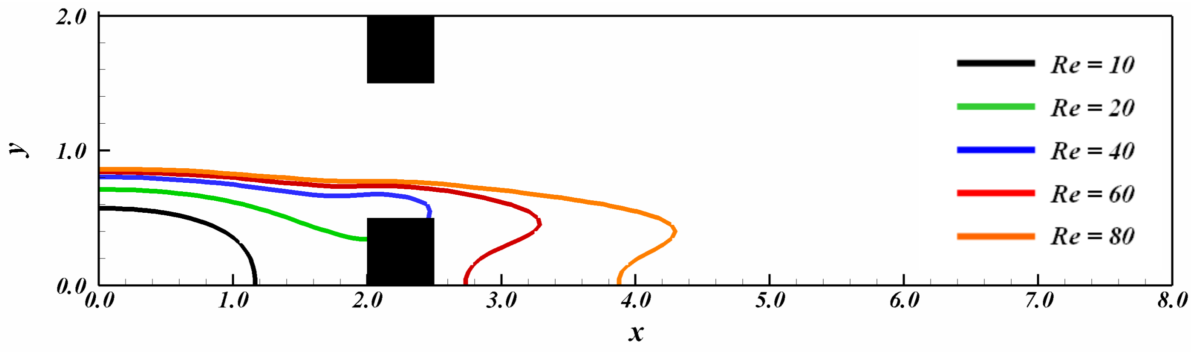

Figure 7. Flame Behavior with obstructions.

4.3. Obstruction geometry effects

The effects of the obstruction geometry, for low Reynolds number, on the flame behavior and on the temperature field are discussed in this subsection. The base case considers the following parameters: $P^*_{obs} = 3$, $H^*_{obs} = 0.25$ and $L^*_{obs} = 1$, $Pr = 0.7$, $Re = 20$, $R_V = 1$ and $R_B = 1$, $D^*_F = 1$, and $L^* = 2$. The thermo-physical properties are chosen as $\Delta H_C = 802$ kJ/mol (Kuo, 1986); $c_p = 30$ J/mol.K; $T_O = 400$ K; $T_F = 300$ K; $Y_{O,in} = 0.233$; $Y_{F,in} = 1$ and $\phi^*_{FO,St} = 0.05518$. The specific heat at constant pressure was considered constant at the average value between the air and the fuel at the nozzles temperatures (Fachini, 2004). The calculated dimensionless adiabatic flame temperature was 15.7 (1869 K).

The cases analyzed in this subsection consider the base case parameter unless the specified ones in each case. The results present in Figs. (8-12) show the temperature field and the flame shape for different obstruction geometries. In Fig. (8), the flame is confined before the obstructions. When the obstructions approach the nozzles, Fig. (9), the flame touches the obstruction.

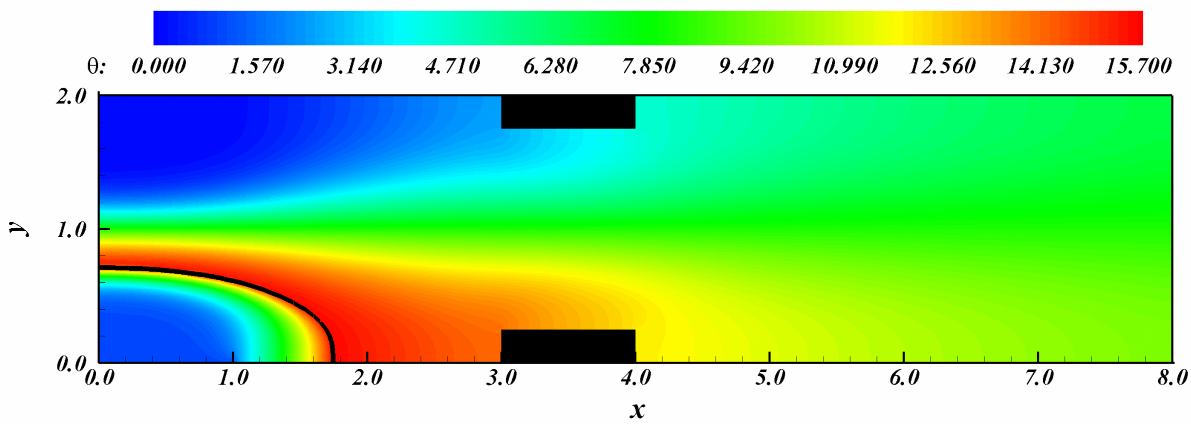

Figure 8. Flame shape and temperature field (base case).

Increasing the obstruction height, the hottest zone is enlarged before the obstructions, as can be seen in Fig. (10).

The Fig. (11) depicts the results for the case with $L^*_{obs} = 2$, but there are not significant differences between this case and the base case. However, when all of the dimensions of the obstruction are increased and the nozzle-obstruction distance is reduced, as shown in Fig. (12), the flame climbs the obstruction and the hottest zone diminishes.

Finally, the Fig. (12) illustrates a triple-modified obstruction set, where the flame is kept confined before the obstructions due to its bigger height in comparison to Fig. (9). It is expected a flow field more strongly affected by the confinement. It is been imposed by this obstruction set, mainly because the proximity with the nozzle inlet region. Besides, a greater mixing effectiveness of the reactants can also be expected, as reported by Wang *et al* (2005).

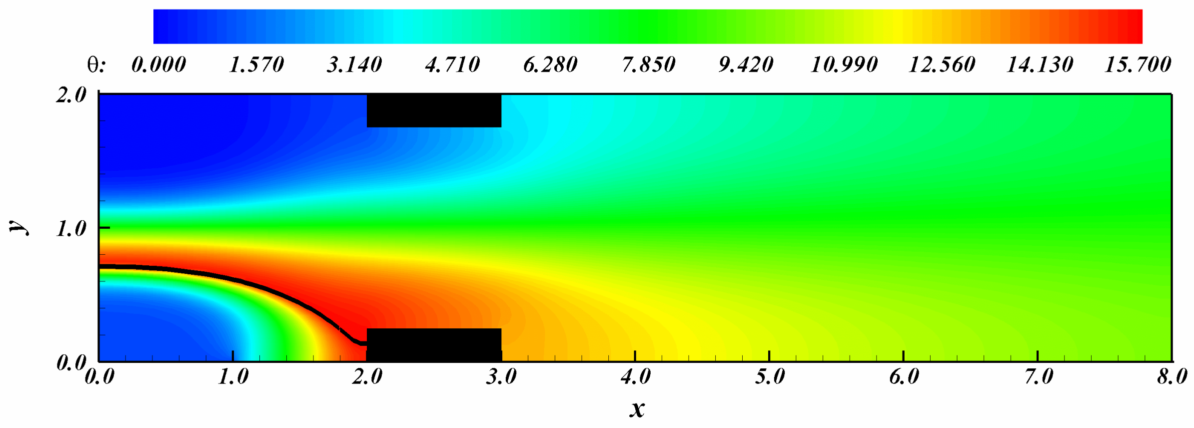

Figure 9. Flame shape and temperature field ($P^*_{obs} = 2$).

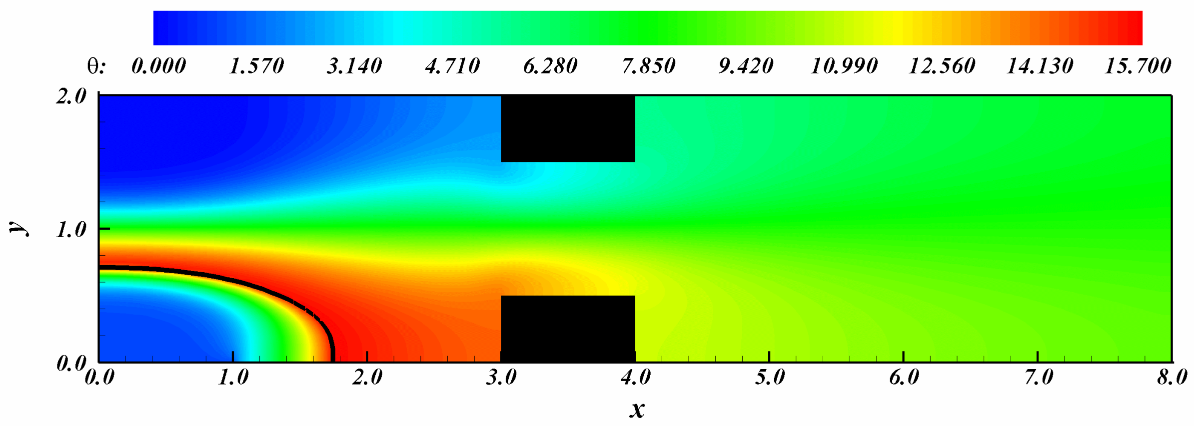

Figure 10. Flame shape and temperature field ($H^*_{obs} = 0.5$).

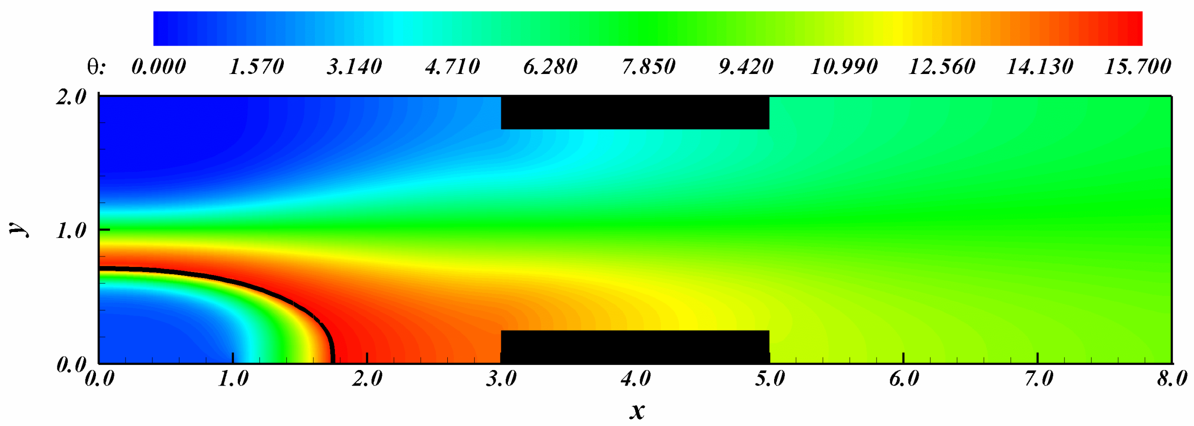

Figure 11. Flame shape and temperature field ($L^*_{obs} = 2$).

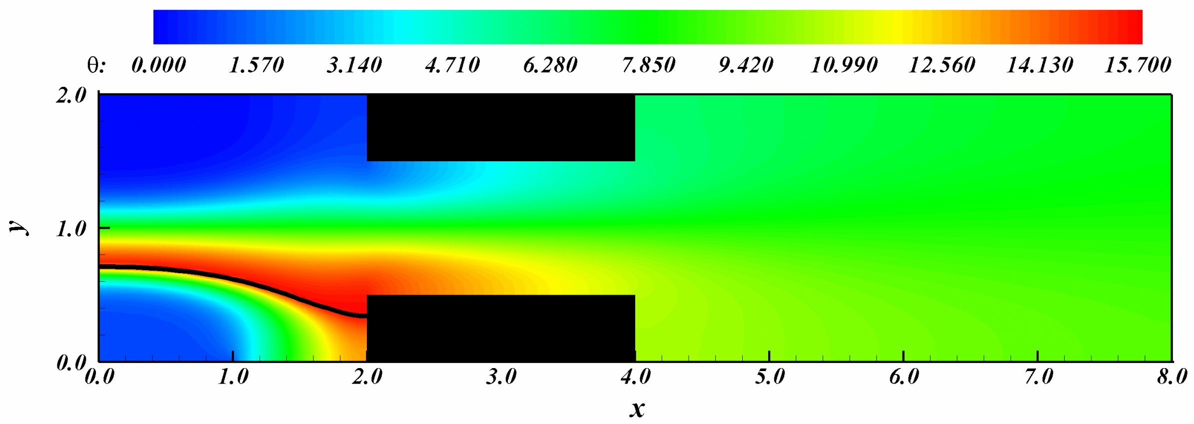

Figure 12. Flame shape and temperature field ($P^*_{obs} = 2$, $H^*_{obs} = 0.5$, $L^*_{obs} = 2$).

5. CONCLUSIONS

The proposed configuration of the confined counterflow with obstructions joins two important mechanisms that influence the flame behavior. The first mechanism is the vortexes zones created in the studied geometry for high Reynolds number and the second one is the adiabatic blockage introduced by the presence of the obstructions that makes difficult the heat transfer process from the region before the obstruction to the region after the obstruction. The last mechanism is more important for small Reynolds number.

For small Reynolds number the obstructions divide the channel in the reaction chamber and discharge channel, because the flame is kept before the obstructions. However, for high Reynolds number it is not observed and the flame is held after the obstruction by the eddy zones. The introduction of the obstructions inside the confined counterflow reduces the flame length and the eddy zones deform the flame as reported by (Roseira Jr and Leiroz, 2005).

The geometry of the obstruction influences the extension of the hottest zone and the flame behavior. Considering the small Reynolds number analysis presented in this work, reducing the nozzle-obstruction distance and increasing the height of the obstruction, simultaneously, the hottest zone is reduced and the flame touches the obstruction.

6. REFERENCES

Amantini, G., Frank, J. H., Smooke, *et al*, 2006, “Computational and Experimental study of Steady Two-dimensional Axisymmetric Non-Premixed Methane Counterflow Flames”, to appear in Combustion Theory and Modeling.

Anderson, D. A., *et al*., 1984, “Computational Fluid Mechanics and Heat Transfer”, New York: Hemisphere Publishing Corporation.

Caldeira, A. B., Rodrigues, R. C. and Leiroz, A., J. K., 2001, “Orifice Plate Effects On Hydrodynamical and Thermal Entrance Regions Inside Flat Channels”, Proceedings of the 16th Brazilian Congress of Mechanical Engineering, CD-ROM, Uberlândia, Brazil, pp. 285-292.

Caldeira, A. B., Leiroz, A. J. K., Orlande, H. R. B., 2005, “Asymmetric Rectangular Obstruction Thermal Effects on Entrance Regions of Flat Plate Cahnnels”, Proceedings of the 18th International Congress of Mechanical Engineering, CD-ROM, Caxambú, Brazil.

Caldeira, A. B., Leiroz, A. J. K., Orlande, H. R. B., 2002, “Rectangular Obstruction Thermal Effects on Entrance Regions of Flat Plate Channels”, Proceedings of the 9th Brazilian Congress of Thermal Engineering and Sciences, CD-ROM, Caxambú, Brazil.

Daou, J. and Liñán, A., 1999, “Ignition and extinction fronts in counterflowing premixed reactive gases”, Combustion and Flame Vol. 118, pp. 479-488.

Esquiva-Dano, I. and Escudie, D., 2005, “A Way of Considering the Influence of Bluff-body’s Geometry on the Non-premixed Flames Stabilization Process”, Combustion and Flame, Vol. 142, pp. 299-302.

Esquiva-Dano, I., Nguyen, H. T. and Escudie, D., 2001, “Influence of Bluff-body’s Shape on the Stabilization Regime of Non-premixed Flames”, Combustion and Flame, Vol. 127, n 4, pp. 2167-2180.

Fachini, F. F., 2001, “N-Fuels Diffusion Flame: Counterflow Configuration”, Proceedings of XVI Congresso Brasileiro de Engenharia Mecânica, CD ROM, Uberlândia, MG, Brazil.

Frouzakis, C. E., Lee, J. C., Tomboulides, D., *et al*, 2002, “From diffusion to premixed flames in an H_2-Air opposed-jet burner: the role of edge flames”, Combustion and Flame, Vol. 130, pp.171-184.

Hanff, E. H. and Campbell, I. G., 2002, “Velocity Field Bimodality in Axisymmetric Diffusion Flame Combustor”, Proceedings of the 12th International Heat Transfer Conference, CD-ROM, Grenoble, France.

Hosseinalipour, S. M., Mujumdar, A. S., 1997, “Flow and thermal characteristics of steady two dimensional confined laminar opposing jets. Part 1: equal jets”, International Communications in Heat and Mass Transfer, No. 24, pp. 27–38.

Hosseinalipour, S. M., Mujumdar, A. S., 1997, “Flow and thermal characteristics of steady two dimensional confined laminar opposing jets. Part 1: unequal jets”, International Communications in Heat and Mass Transfer, No. 24, pp. 39–50.

Kuo, K. K., 1986, “Principles of Combustion”, USA, Wiley-Interscience.

Pellett, G. L., Isaac, K. M., Humphreys, W. M., *et al*, 1998, "Velocity and Thermal Structure, and Strain- Induced Extinction of 14 to 100% Hydrogen-Air Counterflow Diffusion Flames", Combustion and Flame, Vol. 112, No. 4, pp. 575-592.

Roseira Jr, A. P. and Leiroz, A. J. K., 2005, “A Parametric Study of a Confined Stagnation Methane-Air Dfiffusion Flame”, Proceedings of 18th International Congress of Mechanical Engineering, CD ROM, Ouro Preto, MG, Brazil.

Santoro, V. S., Kyritsis, D. C., Gomez, A., 1999, "Extinction Behavior of either Gaseous or Spray Counterflow Diffusion Flames Interacting with a Laminar Toroidal Vortex", 17th International Colloquium on the Dynamics of Explosions and Reactive Systems, Heidelberg, Germany.

Tsuji, H., 1982, “Counterflow Diffusion Flames”, Progress Energy Combustion Science, Vol.8, pp. 93-119.

Wang, S. J., Devahastin, S., Mujumdar, A. S., 2005, “A numerical investigation of some approaches to improve mixing under laminar confined impinging streams”, Appl. Therm. Eng. No. 25, pp. 253–269.

Wang, S. J., Mujumdar, A. S., 2006, “Flow and mixing characteristics of multiple and multi-set opposing jets”, Chem. Eng. and Process, *in press*.

Williams, B. A., 2001, “Sensitivity of calculated extinction strain rate to molecular transport formation in non-premixed counterflow flames”, Combustion and Flame, Vol. 124, pp. 330–333.

Williams, F. A., 1985, “Combustion Theory”, 2nd ed., Ed. Adison Wesley, USA.